Sensing and Bio-Sensing Research 4 (2015) 30–36

Contents lists available at ScienceDirect

Sensing and Bio-Sensing Research

journal homepage: www.elsevier.com/locate/sbsr

Detection of *S*-nitrosylated protein by surface plasmon resonance

Ruirui Wang, Qingnan Kong, Jie Zhou, Lili Zhang *, Shuhua Zhu *

College of Chemistry and Material Science, Shandong Agricultural University, Taian, Shandong 271018, China

ARTICLE INFO

Keywords:
Surface plasmon resonance
Nitric oxide
S-Nitrosylated protein
Biotin–streptavidin

ABSTRACT

S-Nitrosylation has recently emerged as an important posttranslational modification of proteins and is becoming an intensive field of research in plants. Protein *S*-nitrosation, a reversible post-translation modification of cysteine, affects many cell signaling pathways and plays critical roles in redox-sensitive cell signaling. Changes in protein function effectively transmit biological signals and thus provide a framework for elucidating signaling networks. This paper presented a new, universal immunosensor for detection of *S*-nitrosylated proteins. Electrochemical impedance spectroscopy (EIS) and atomic force microscope (AFM) were used to estimate the formation of self-assembled film. This method was based on the specific binding characteristics of biotin–streptavidin, using Biotin-HPDP labeled protein sulfhydryl group as the substrate to detect proteins. The sensor was used to detect bovine serum albumin (BSA), nitrosylated BSA and denitrosylated BSA. The results showed that 90.61% of nitrosylated BSA were reduced, verifying that protein *S*-nitrosylation is a reversible and effective post-translation modification. This method was successfully applied to detect *S*-nitrosylated protein in Feicheng peach. The results showed good repeatability and precision. This method provided a molecular basis for further exploring the mechanism of *S*-nitrosylation of proteins in plants.

1. Introduction

S-Nitros(yl)ation is a reversible modification of free cysteine residues mediated by nitric oxide (NO), resulting in generation of *S*-nitrosothiols. NO can react with thiol group of cysteine residues to form *S*-nitrosothiols (*S*-nitrosylation) [1,2]. *S*-Nitrosylation was thought to be controlled principally through the regulation of NO biosynthesis. Emerging evidences, however, indicate that nitrosothiol (SNO) turnover may provide an alternative regulatory mechanism [3,4]. *S*-Nitrosylation of the antioxidant tripeptide glutathione forms *S*-nitrosoglutathione (GSNO), which is thought to function as a mobile reservoir of NO bioactivity [5]. During the past few years, *S*-nitrosylation, the covalent and reversible binding of NO to the thiols of reduced reactive cysteine residues, has emerged as an important posttranslational modification [6]. *S*-Nitrosylation is thought to account for much of the widespread influence of NO on cellular signaling through redox-based biochemical regulation of signaling component [7,8]). Protein *S*-nitrosylation can produce a labile *S*-nitrosothiol structure and some functional alterations, containing a broad range of physiological and pathological cellular instances [9,10].

There are some techniques to detect *S*-nitrosylated protein, including UV–Vis spectroscopy [11], electrochemistry [12,13], Biotin switch method [14], high performance liquid chromatography–tandem mass spectroscopy (HPLC–MS) [15,16], Gold nanoparticle enrichment technique [17] and fluorescence labeling method [18]. However, these methods for detection *S*-nitrosylated protein seem to be insufficient. The method of UV–Vis spectroscopy is simple, but has many disturbing components. There are a lot of advantages of electrochemical method to monitor *S*-nitrosylation, which can obtain higher sensitivity, accuracy and wider measuring range compared to other methods. However, many disadvantages, such as long time and poor repeatability, make it significantly more difficult to perform. Biotin switch method is relatively effective and sensitive, but this method may produce false negative results. Fluorescein labeling method has the advantage of saving time, can qualitatively analyze single pure but not mixture samples, and fails to determine the site of *S*-nitrosylation.

Surface plasmon resonance (SPR), a surface-sensitive detecting technique based on changes in refractive index (RI), can be used to measure the changes occurring on the thin metal films as a result of recognition events or chemical reactions [19,20]. Owing to its features of simplicity, low cost, non-labeling, high-sensitivity and real-time measurement, SPR monitoring has received much interest from scientific community [21–24]. This interesting technique has become a widely method used to monitor protein

* Corresponding authors. Tel.: +86 538 8246369; fax: +86 538 8242251 (L. Zhang). Tel.: +86 538 8247790; fax: +86 538 8242251 (S. Zhu).

E-mail addresses: huaxue79@163.com (L. Zhang), shuhua@sdau.edu.cn (S. Zhu).

http://dx.doi.org/10.1016/j.sbsr.2015.02.001

binding, drug screening, environmental contaminants and biochemical reactions [25–28]. In this paper, a simpler and more selective method for detection *S*-nitrosylated proteins by using SPR technology were established and successfully applied to analyze the protein *S*-nitrosylation in peach fruit.

2. Material and methods

2.1. Material

Biotin-HPDP and 11-mercaptoundecanoicacid (COOH-tin) were purchased from Sigma. Bovine serum albumin (BSA) was from Roche. HRP-streptavidin was obtained from the Beyotime Biotechnology (China). N-hydroxysuccinimide (NHS), sodium ascorbate, ethanolamine hydrochloride, and N-ethyl-N′-(3-diethylaminopropyl) carbodiimide (EDC) were purchased from Aladdin Chemistry CO. Ltd. All other reagents and solvents were analytical reagent grade and MilliQ-grade water was used. All solutions were filtered with 0.22 mm microfiltration membrane and thoroughly degassed prior to use.

2.2. Preparation of SPR biosensor

Immobilization of COOH-tin on gold surface was carried out according to the procedure published previously [29,30]. The gold-sputtered slide glass, as a sensor chip, was dipped in 10 mL of freshly prepared piranha solution (70% H_2SO_4, 30% H_2O_2) for 10 min, rinsed with anhydrous ethanol and copious distilled water, then placed into 20 mL of 1.0 mmol L^{-1} COOH-tin in ethanol, and kept at 4 °C overnight. The surfaces of gold-sputtered slide glass were washed with absolute ethanol and super-pure water before being dried under a stream of nitrogen, and then placed in 0.1 mol L^{-1} sodium phosphate buffer (PBS) (pH 7.4, including 0.2 mol L^{-1} EDC and 0.05 mol L^{-1} NHS) for 20 min to activate the carboxyl groups into reactive N-hydroxysuccinimate esters. After rinsed, the gold plate was immersed in 20 mL of 0.1 mol L^{-1} PBS buffer (pH 7.4, containing 0.1 g L^{-1} streptavidin) for 24 h at room temperature, and then rinsed thoroughly with distilled water. Ethanolamine solution (1 mol L^{-1}) was used to deactivate and block the unreacted esters and desorb the electrostatic bound proteins or other small molecules. During the final step, the gold substrate was submerged in 20 mL of 0.1 mol L^{-1} PBS buffer (pH 7.4, containing 0.1 g L^{-1} Biotin-HPDP) overnight at ambient temperature. Thus the surface-grafted film on a gold-sputtered slide glass was formed.

2.3. FT-SPR experiments

The Fourier transform-surface plasmon resonance (FT-SPR) measurements were performed with an SPR-100 module (Thermo) equipped with a flow sample cell mounted on a goniometer, which was inserted in a Thermo Nexus FT-IR spectrometer with a near-IR tungsten–halogen light source. The incidence angle was adjusted to have minimal reflectivity located at 9000 cm^{-1} at the beginning of each experiment so as to be in the best sensitivity region of the Indium Gallium Arsenide (InGaAs) detector. A peristaltic pump was used to pump the analyte or wash solution from a reservoir into the flow cell. PBS buffer (0.1 mol L^{-1}, pH 7.4) was used as running buffer, and the flow rate was 1.20 mL min^{-1}. Different concentrations of tested compounds dissolved in the running buffer were injected into the flow cell until the wavenumber shifts reached stable values. The stable wavenumber shifts were recorded in real time using the FT-SPR. Before each binding measurement for the sample solutions, the SPR sensor chips were washed with PBS buffer (0.1 mol L^{-1}, pH 7.4) in turn until a stable base line was obtained. The data (shown as a wavenumber shift in SPR angle) were expressed as the wavenumber shift in SPR angle of sample subtracting the background data of PBS (0.1 mol L^{-1}, pH 7.4) from those obtained from sample solutions. The average of five replicated measurements was obtained for each sample. Most of solutions were ultrasonicated in all the experiments.

2.4. AFM measurements

Atomic force microscopy (AFM) was demonstrated with a dimension icon scan probe microscopy (Veeco Instruments Inc, America) to study the surface morphologies of the SPR chip in tapping mode. All AFM images were obtained by NanoScope Analysis.

2.5. Electrochemical measurements

Cyclic voltammogram (CV) and alternating current impedance experiments were done on CHI 660A workstation (Shanghai Chenhua Instruments Company, China). A conventional three-electrode electrochemical system, with modified Au chip as working electrode, a platinum wire as counter electrode and a saturated calomel electrode (SCE) as the reference electrode, was used to measure the electrochemical response. The electrochemical measurements were performed in 0.1 mol L^{-1} PBS (pH 7.0, containing 10 mmol L^{-1} $[Fe(CN)_6]^{3-/4-}$and 1 mol L^{-1} KCl) at room temperature.

Gold disk electrode (1-mm diameter) was used for electrochemical impedance measurements. The electrode were pretreated as described in the previous work and form a monolayer of 10^{-3} mol L^{-1} COOH-tin by immediately immersing a cleaned gold electrode in a solution of COOH-tin in absolute ethanol [31]. And the multilayer construction was performed according the same procedure as described previously in preparation of SPR biosensor section [32].

2.6. Sample preparation

Peach fruits (*Prunus persica* (L.) Batsch, cv. Feicheng) picked from Feicheng Shandong province in China at mature stage, were treated by scavenge c-PTIO, nitric oxide (5 μmol L^{-1} NO, 15 μmol L^{-1} NO, 30 μmol L^{-1} NO), respectively. The fruit treated with distilled water used as the control (CK). All the fruits were frozen immediately in liquid nitrogen and stored at −80 °C. Mitochondria were isolated from peach fruits at 0–4 °C [33]. Mesocarps of peach fruits (10 g) were homogenized with 20 mL of 25 mmol L^{-1} Mops-KOH (pH 7.8, containing 0.4 mol L^{-1} D-mannitol, 1 mmol L^{-1} EGTA, 10 mmol L^{-1} tricine, 8 mmol L^{-1} L-cysteine, 0.1% BSA, 1% PVP) at 4 °C for about 20 min. Then the homogenates were filtered through 6 layers of cheese cloth. The filtrates were centrifuged at 3000×*g* and 4 °C for 5 min. The supernatants were then centrifuged at 16,000×*g* and 4 °C for 25 min. The pellets were resuspended with 2 mL of 10 mmol L^{-1} Mops-KOH buffer (pH 7.2, including 0.4 mol L^{-1} D-mannitol, 1 mmol L^{-1} EGTA, 0.1% BSA), and centrifuged at 16,000×*g* and 4 °C for 30 min. The pellets were collected as crude mitochondria. The crude mitochondria were purified by sucrose step density gradient centrifugation [34]. The purified mitochondria were resuspended with 1 mL 0.1 mol L^{-1} PBS buffer (pH 7.4) and disrupted by ultrasonator (JY92-IID, Ningbo Xinzhi Co. Ltd, China) for the following experiments. In a preliminary step of the procedure, free thiols of protein were blocked by methylthiolation with 0.02 mol L^{-1} methyl methanethiosulfonate (MMTS). This modification can be reversed by reduction with 2-mercaptoethanol (2-ME). Unreacted MMTS was removed in a subsequent step either by filtering the protein mixture through a spin column (Micro Bio-Spin P6,

Bio-Rad) or by acetone precipitation. In the final step, nitrosothiols were selectively reduced with ascorbate (0.05 mol L^{-1}) to reform the thiol [35]. The free thiols of protein were detected by FT-SPR technique.

3. Results and discussion

3.1. Immobilization of the BSA onto biotin/streptavidin/COOH-tin/Au surface

BSA, as an acidic single polypeptide protein with molecular weight of 66.4 kDa, has been used extensively in the pharmaceutical industry for a variety of applications. BSA is selected as the protein model because of its low cost, ready availability, and unusual ligand-binding properties. BSA is constituted by 582 amino acid residues, of which 35 cysteines compose 17 disulfide bonds. There is only one free hydrosulphonyl, which can be used as substrate to detect *S*-nitrosylated protein. The formation process of the multilayer was as follows: Firstly, one layer of COOH-tin was immobilized on bare gold by Au–S bond. Secondly, the layer of streptavidin was immobilized on the self-assembled monolayer of carboxyl terminated alkanethiol on the gold surface using EDC and NHS as activators [36]. Thirdly, Biotin-HPDP was specifically bound to streptavidin/COOH-tin/Au surface. Finally, BSA reacted with Biotin-HPDP to produce stabilized disulfide bond, thereby immobilized onto biotin/streptavidin/COOH-tin/Au surface [37–39]. Self-assembly process was given in Scheme 1.

3.2. SPR study of multilayer formation

To verify whether the self-assembled films were immobilized on the surface of the gold substrates, the FT-SPR spectra on bare gold, COOH-tin modified films and streptavidin/COOH-tin/Au films in contact with 0.1 mol L^{-1} PBS buffer (pH 7.4) were measured by SPR at room temperature, respectively (Fig. 1). The wavenumber shifts of 124 cm^{-1} and 142 cm^{-1} were observed onto the COOH-tin modified films and streptavidin modified Au surfaces,

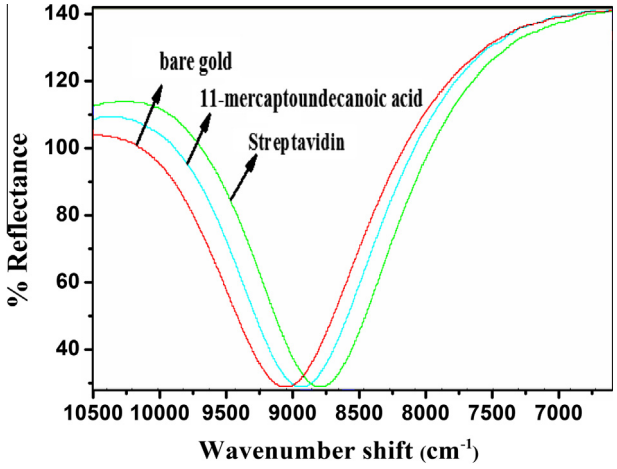

Fig. 1. Characteristics of SAM.

respectively. This result certified the formation of the molecularly self-assembled layer on the gold surface [31].

3.3. AFM measurements

AFM was used to characterize the surface self-assembly film of the BSA/biotin–streptavidin/COOH-tin/Au films. Images obtained in air using a NanoScope IIIa (Digital Instruments) in tapping mode with standard silicon cantilevers had a normal spring constant of 28 nm^{-1} (Fig. 2). The morphology of bare gold had a smooth surface. However, after immobilization of COOH-tin, the increase in surface roughness indicated that a COOH-thiol monolayer formed on a gold surface. The following immobilization of streptavidin and Biotin-HPDP, the enlargement of particle compactness on gold surface demonstrated streptavidin and Biotin-HPDP onto the COOH-tin/Au, and the presence of a uniformly distributed

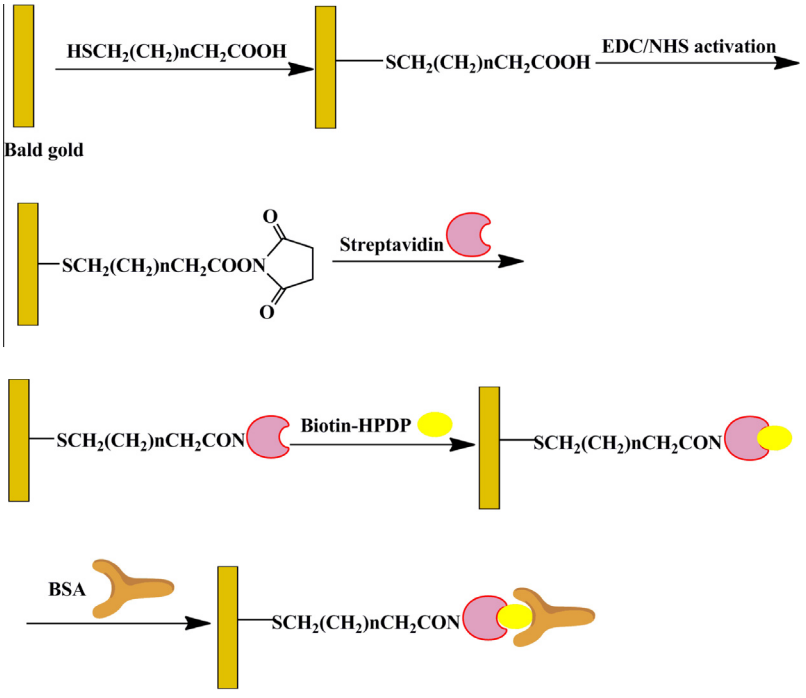

Scheme 1. Schematic of covalent immobilization of BSA on biotin/streptavidin/COOH-tin/Au SAM.

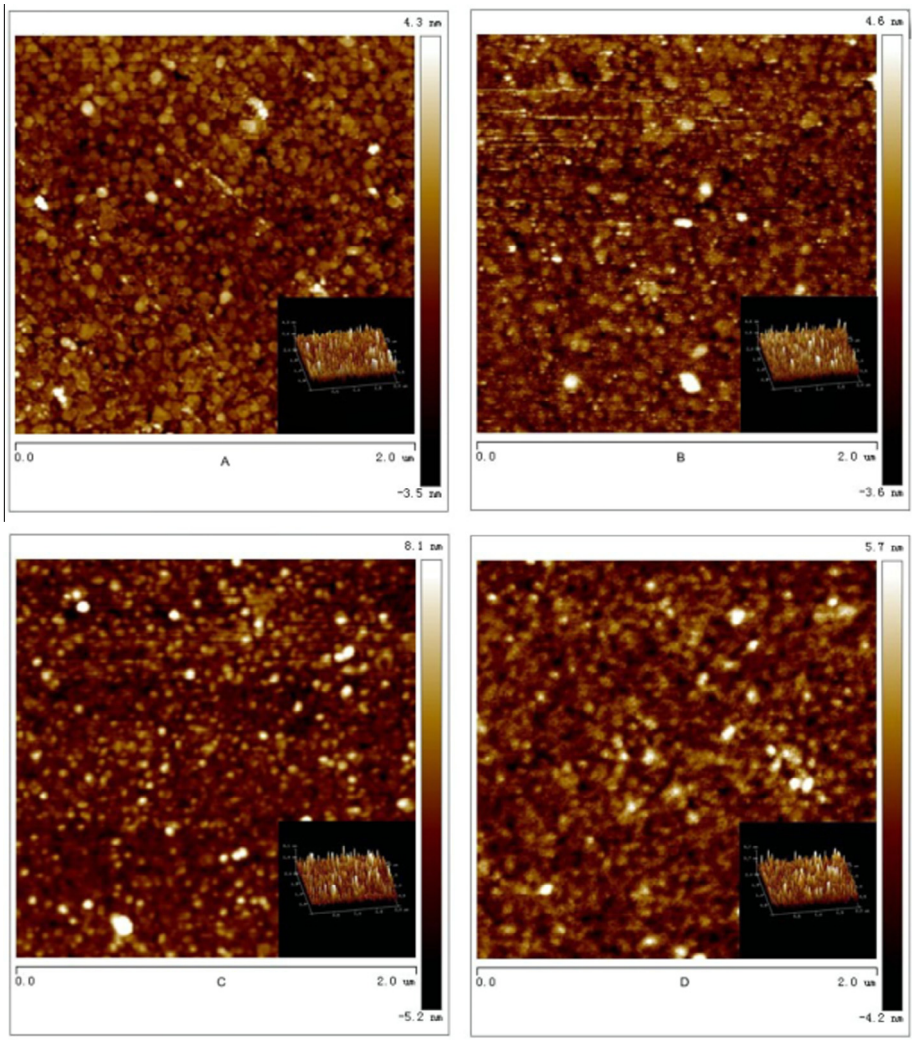

Fig. 2. Topography 2D images with 3D insets obtained by AFM, (A) bare gold, (B) COOH-tin/Au, (C) streptavidin–biotin/COOH-tin/Au, (D) BSA/biotin-streptavidin/COOH-tin/Au.

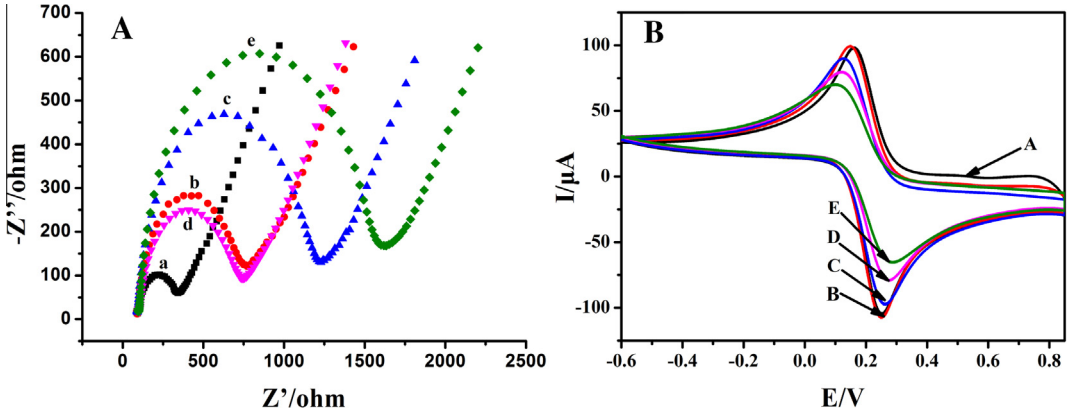

Fig. 3. (A) Impedance spectra of Au (a), COOH-tin/Au (b), streptavidin/COOH-tin/Au (c), biotin/streptavidin/COOH-tin/Au (d), BSA/biotin/ streptavidin/COOH-tin/Au (e) in 10 mmol L^{-1} $K_3Fe(CN)_6$ and 1 mol L^{-1} KCl solution. (B) Cyclic voltammograms of Au (A), COOH-tin/Au (B), streptavidin/COOH-tin/Au (C), biotin/streptavidin/COOH-tin/Au (D), BSA/biotin/ streptavidin/COOH-tin/Au (E) in10 mmol L^{-1} $K_3Fe(CN)_6$ and 1 mol L^{-1} KCl solution. The accumulation time and scan rate were 5 s and 100 mV/s, respectively.

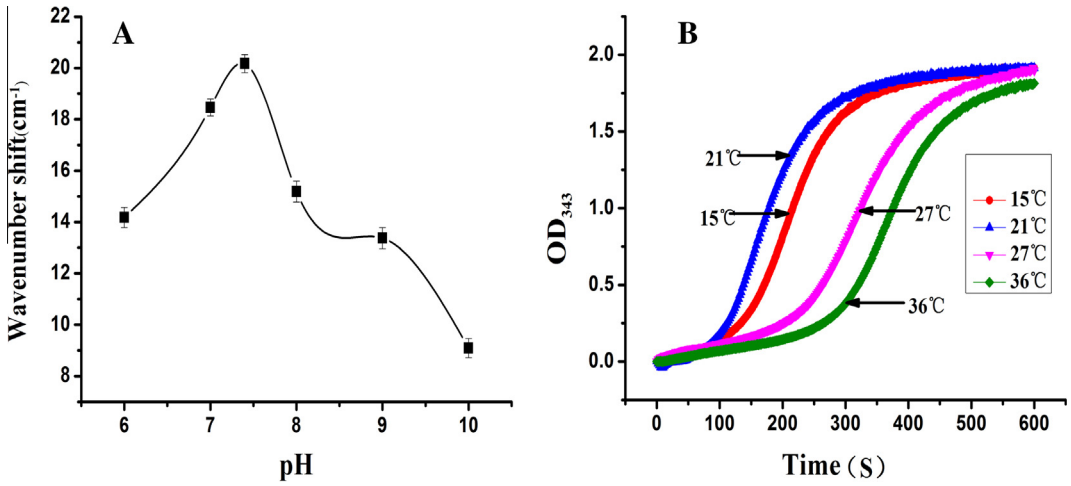

Fig. 4. (A) The influence of pH on the performance of streptavidin combined with gold. (B) The dynamics curve of Biotin-HPDP and BSA.

structure indicated the immobilization of BSA onto the biotin–streptavidin/COOH-tin/Au electrode [40,41].

3.4. Electrochemical impedance spectroscopy

Electrochemical impedance spectroscopy (EIS) is a highly effective method for investigating the features of a surface-modified electrode using the redox probe $[Fe(CN)_6]^{3-/4-}$ [42,43]. In this study, EIS was carried out to explore the changes in charge transfer resistance (Rct) that aroused from every surface modification step as shown in Fig. 3A. The value of Rct, charge-transfer resistance, obtained as 780 Ω (b) for COOH-tin/Au was bigger than that of the bare gold electrode (260 Ω) (a). This result could be attributed to the pulsion between the negative charge of the COOH-tin with terminal carboxyl groups on the electrode surface and $[Fe(CN)_6]^{3-/4-}$ in solution resulting in the reduction of electron charge or increase of resistance to the flow of electrons. From Fig. 1A(c), it is apparent that the Rct increased dramatically to about 1200 Ω, which proved the higher steric hindrance – the amount of ferri/ferrocyanide ions approached to the electrode surface was decreased after binding of streptavidin. Because streptavidin was nonconductive, electron-transfer of $[Fe(CN)_6]^{4-/3-}$ was blocked by the multilayer film. In the following amplified steps by adsorption of Biotin-HPDP, the value of Rct was obtained with 760 Ω (d). This result might be attributed to the presence of redox couples present in the solution. Moreover, the nitrogen atom in the pyridyl was powerful, and had high electron-withdrawing property, so the electrode surface impedance value decreased. The electrode surface was coated with BSA. It could be seen that the interfacial electron transfer resistance was amplified from 760 (d) to1700 Ω (e). Compared to the earlier steps, the value of Rct in the last process was largest, which suggested that the effect of amplification was very obvious.

3.5. Cyclic voltammetric response studies

CV is also an effective way to explore the characterization of a surface-modified electrode. As shown in Fig. 3B, the redox peak currents were: BSA < SA < COOH-tin < Biotin-HPDP < blank gold. These results were consistent with EIS. Depending on the results of EIS and CVs, it could be seen that the electrode was fabricated by layer-by-layer modification.

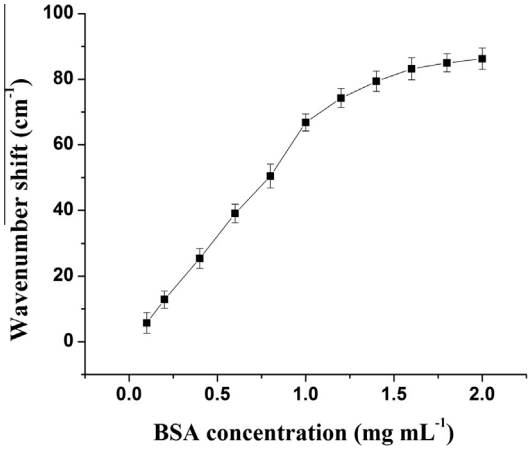

Fig. 5. The determination of different concentration of BSA.

Table 1
Reaction rate between Biotin-HPDP and BSA.

Temperature (°C)	15	21	27	36
Velocity (mol mol^{-1})	1.3015	1.9128	1.5709	0.734

3.6. Effects of pH on the performance of streptavidin combined with gold

According to the literatures [31], using PBS buffer as the experiment buffer system, the effect of pH on the performance of streptavidin assembled onto gold surface was studied by varying the pH in the range of 6.0–10.0. Fig. 4A showed that the wavenumber shifts increased from pH 6.0 to 7.4, and reached the maximum at pH 7.4. However, when the pH values ranged from 7.4 to 10.0, the adsorption of streptavidin on the COOH-tin film decreased. The phenomenon could be explained by the fact that under neutral and alkaline environment, carboxyl was activated by EDC/NHS with negative electricity, and could utilize electrostatic adsorption to make proteins gather on biosensors. As a result, pH of the PBS solution should be lower than the isoelectric point of protein, which facilitated streptavidin combining into gold surface. Hence, the pH of PBS buffer was adjusted to 7.4 for all of the experiments.

3.7. Effect of temperature on interaction between Biotin-HPDP and BSA

The chemical reaction between Biotin-HPDP and hydrosulphonyl would generate pyridine-2-ketone of sulfur, which had specific absorption peak at 340 nm. Fig. 4B revealed the kinetic reaction between Biotin-HPDP and BSA at different temperature. Through real-time monitoring of OD_{343} changes, the kinetics of reaction between Biotin-HPDP and BSA were studied. Fig. 5 demonstrated that the reaction reached equilibrium after 600 s, OD_{343} also achieved maximum and no longer changed after 600 s. The result indicated that the optimum time of the Biotin-HPDP reaction with BSA was 600 s. As bioactive molecule, protein interaction was influenced by temperature. The reaction kinetics curves were studied at different temperatures, and the reaction velocity was in Table 1.

Table 1 showed the reaction rate reached the maximum at 21 °C, and at the temperature the reaction reached equilibrium firstly. As a result, the optimum temperature was 21 °C of the four temperatures above.

3.8. SPR detection of different concentration of BSA

A range of different concentrations of BSA were detected by SPR technique, and a very good linearity from 0.1 to 1.0 mg mL^{-1} in the range of the tested BSA concentration was found ($R = 0.998$). With BSA concentration increasing, the specific binding sites between Biotin-HPDP and BSA would reach saturation. However, the non-specific binding resulted in a non-quantitative relationship between the substrate molecule and the specific binding sites.

3.9. S-Nitrosation of BSA nitrosylated by S-nitrosoglutathione (GSNO)

Transnitrosation reactions in which an NO^+ (nitrosonium ion) group is directly transferred from a *S*-nitrosated protein (PSNO) or a low-molecular-weight RSNO, such as GSNO [44], to another protein thiol can lead to protein *S*-nitrosation. BSA *S*-nitrosation can result from transnitrosation reactions induced by GSNO. In order to further present BSA was nitrosylated to what extent and prove hydrosulphonyl specificity combination of the BSA, three experiments were designed: (i) control, BSA (ii) BSA + GSNO, BSA (1 mg mL^{-1}) was were treated with 1 mmol L^{-1} GSNO (iii) BSA + GSNO + DTT, nitrosylated BSA were reduced by reducing reagent DL-Dithiothreitol (DTTS).

Fig. 6A demonstrated that the wavenumber shifts caused by BSA solution of 1 mg mL^{-1} in 0.1 mol L^{-1} PBS buffer was 68.743. The wavenumber shifts caused by BSA + GSNO was 19.295, wavenumber shifts declined 71.93% compared to the control. The results suggested that most of the free thiol residues of BSA were nitrosylated by GSNO. In other words, 71.93% of BSA occurred *S*-nitrosation. However, the modification was reversible. The wavenumber shifts caused by BSA + GSNO + DTT solution in 0.1 mol L^{-1} PBS buffer was 62.287, of which 90.61% of nitrosylated BSA were reduced with DTT treatment, and got sulfur free residue. The results indicated *S*-nitros(yl)ation was the reversible NO-mediated modification of free cysteine residues.

3.10. Detection of S-nitrosylated protein in peach fruit

In order to demonstrate the applicability of the coupled method for analysis of the real samples, the sensor was used to detect *S*-nitrosylated proteins from different treatment peach fruits. *S*-Nitrosylated protein was reduced by ascorbate to re-form thiol that was combined with Biotin-HPDP instead of BSA, thus the SPR response was obtained. As shown in Fig. 6B, the wavenumber shifts caused by the control of peach fruits was 103.2115. The wavenumber shifts caused by c-PTIO of peach fruits was 99.13867, which wavenumber shifts decreased by 4.07283 compared to that of the control (103.2115). The wavenumber shifts caused by 5 μmol L^{-1} NO of peach fruits was 120.2557, which wavenumber shifts increased by 16.9407 compared to control (103.2115). The wavenumber shifts caused by 15 μmol L^{-1} NO of peach fruits was 136.0763, which wavenumber shifts increased by 35.8613 compared to the control (103.2115). The wavenumber shifts caused by 30 μmol L^{-1} NO of peach fruits was 108.0357, which was only 79.34% that of the treatment with 15 μmol L^{-1} NO. The free sulfhydryls, which were released by *S*-nitrosylated protein of peach fruits pretreated with NO, showed a significant increase in wavenumber shifts compared to the control. Whereas, the wavenumber shifts that caused by free sulfhydryls from the *S*-nitrosylated protein of peach fruits pretreated with c-PTIO was least than that of other treatments. The results suggested that NO could promote the *S*-nitrosylation of proteins and the protein *S*-nitrosylation was prevented by c-PTIO. Treatment with 15 μmol L^{-1} NO caused the maximum wavenumber change, while the wavenumber shift showed downward trends caused by the treatment with 30 μmol L^{-1} NO. The results also indicated that the nitrosation functions of protein sulfhydryl groups would be inhibited if NO concentration was high. Universality and simplicity of performing the test would not only allow its application for detection method in fruits, but also in plants and animals.

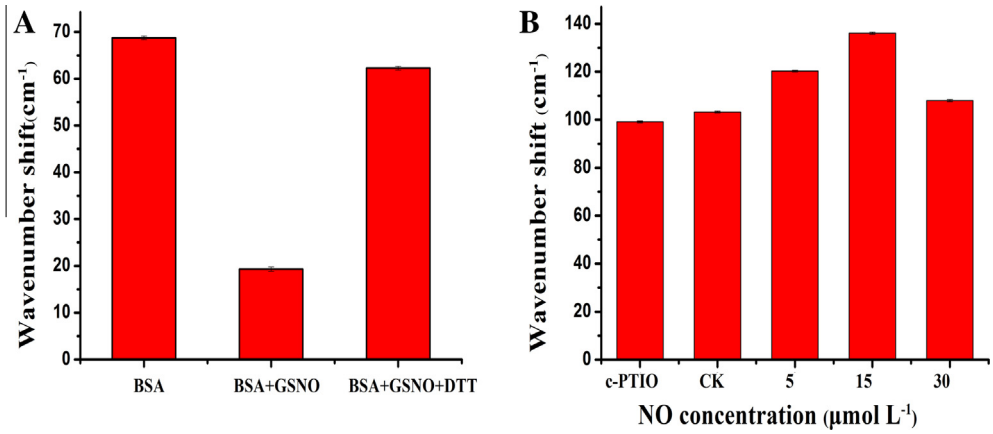

Fig. 6. (A) The reference experiment of GSNO. (B) The determination of real samples.

4. Conclusion

In this study, a universal SPR sensor was constructed for the detection of *S*-nitrosylated protein using streptavidin and Biotin-HPDP as signal amplification elements. The formation of multilayer was detected in real time based on SPR. EIS and AFM were also used to characterize the formation of multilayer. The results from the biosensor effectively indicated *S*-nitrosation was the reversible NO-mediated modification of free cysteine residues. This method was successfully utilized to estimate *S*-nitrosylated protein of peach fruits. The results indicated that NO could promote the *S*-nitrosylation of proteins. With the concentration of NO increasing, *S*-nitrosylation of proteins in peaches enhanced. If the concentration of NO was too high, the *S*-nitrosylation of peach fruits would be inhibited. The method for the detection of *S*-nitrosylated protein in real samples offered good accuracy, high sensitivity and selectivity, which can provide a technology for further study on *S*-nitrosation.

Conflict of interest

There is no conflict of interest.

Acknowledgements

This work was supported by National Natural Science Foundation of China (Nos. 31270723, 31370686, 31470686), Natural Science Foundation of Shandong Province (ZR2013CQ014), Youth Science and Technology Innovation Fund of Shandong Agricultural University and Science and Technology Development Planning of Shandong Province, China (2013GZX20109).

References

[1] J. Durner, Nitric Oxide 27 (2012) S9.
[2] A. Feechan, E. Kwon, B.W. Yun, Y. Wang, J.A. Pallas, G.J. Loake, Proc. Natl. Acad. Sci. USA 102 (2005) 8054–8059.
[3] B. Kolesnik, K. Palten, A. Schrammel, H. Stessel, K. Schmidt, B. Mayer, A.C.F. Gorren, Free Radic. Biol. Med. 63 (2013) 51–64.
[4] A. Lin, Y. Wang, J. Tang, P. Xue, C. Li, L. Liu, B. Hu, F. Yang, G.J. Loake, C. Chu, Plant Physiol. 158 (2012) 451–464.
[5] H. Wunsche, I.T. Baldwin, J. Wu, J. Exp. Bot. 62 (2011) 4605–4616.
[6] D.D. Thomas, D. Jourd'heuil, Antioxid. Redox Signal. 17 (2012) 934–936.
[7] M.J. Kohr, A.M. Evangelista, M. Ferlito, C. Steenbergen, E. Murphy, J. Mol. Cell. Cardiol. 69 (2014) 67–74.
[8] R. Sengupta, A. Holmgren, Biochim. Biophys. Acta 1820 (2012) 689–700.
[9] K.Y. Rhee, H. Erdjument-Bromage, P. Tempst, C.F. Nathan, Proc. Natl. Acad. Sci. USA 102 (2005) 467–472.
[10] F. Torta, V. Usuelli, A. Malgaroli, A. Bachi, Proteomics 8 (2008) 4484–4494.
[11] L. Zhukova, I. Zhukov, W. Bal, A. Wyslouch-Cieszynska, Biochim. Biophys. Acta, Cell Res. 1742 (2004) 191–201.
[12] M.J. Kohr, A.M. Aponte, J. Sun, G. Wang, E. Murphy, M. Gucek, C. Steenbergen, Am. J. Physiol. Heart Circ. Physiol. 300 (2011) H1327–H1335.
[13] J.B. Mannick, C.M. Schonhoff, in: C. Enrique, P. Lester (Eds.), Methods in Enzymology, Academic Press, 2008, pp. 231–242.
[14] S.R. Jaffrey, S.H. Snyder, Sci. Signal. 2001 (2001) pl1.
[15] M.T. Forrester, J.W. Thompson, M.W. Foster, L. Nogueira, M.A. Moseley, J.S. Stamler, Nat. Biotechnol. 27 (2009) 557–559.
[16] B. Shen, A.M. English, Biochemistry 44 (2005) 14030–14044.
[17] A. Faccenda, C.A. Bonham, P.O. Vacratsis, X. Zhang, B. Mutus, J. Am. Chem. Soc. 132 (2010) 11392–11394.
[18] J.E. Wiktorowicz, S. Stafford, H. Rea, P. Urvil, K. Soman, A. Kurosky, J.R. Perez-Polo, T.C. Savidge, Biochemistry 50 (2011) 5601–5614.
[19] M. Riskin, R. Tel-Vered, I. Willner, Adv. Mater. 22 (2010). 1387-1387.
[20] Q.Q. Wei, T.X. Wei, Chin. Chem. Lett. 22 (2011) 721–724.
[21] V. Banerjee, K.P. Das, Colloids Surf. B 111 (2013) 71–79.
[22] A. Boulkroune, N. Bounar, M. M'Saad, M. Farza, Neurocomputing 135 (2014) 378–387.
[23] E. De Juan-Franco, J.M. Rodríguez-Frade, M. Mellado, L.M. Lechuga, Talanta 114 (2013) 268–275.
[24] R. Gordon, D. Sinton, K.L. Kavanagh, A.G. Brolo, Acc. Chem. Res. 41 (2008) 1049–1057.
[25] M. Frasconi, R. Tel-Vered, M. Riskin, I. Willner, Anal. Chem. 82 (2010) 2512–2519.
[26] R.B. Pernites, R.R. Ponnapati, R.C. Advincula, Macromolecules 43 (2010) 9724–9735.
[27] M. Riskin, R. Tel-Vered, I. Willner, Adv. Mater. 22 (2010) 1387–1391.
[28] K. Wybranska, W. Niemiec, K. Szczubiałka, M. Nowakowska, Y. Morishima, Chem. Mater. 22 (2010) 5392–5399.
[29] L.K. Ista, S. Mendez, V.H. Pérez-Luna, G.P. López, Langmuir 17 (2001) 2552–2555.
[30] N. Zhao, C. Chen, J. Zhou, Sens. Actuators B 166–167 (2012) 473–479.
[31] C. Zhou, J. Gao, L. Zhang, J. Zhou, Anal. Chim. Acta 812 (2014) 129–137.
[32] X. Cui, R. Pei, Z. Wang, F. Yang, Y. Ma, S. Dong, X. Yang, Biosens. Bioelectron. 18 (2003) 59–67.
[33] A.H. Millar, A. Liddell, C.J. Leaver, Method. Cell Biol. 80 (2007) 65–90.
[34] D.A. Clayton, G.S. Shadel, Cold Spring Harbor Protocols 2014, pdb. prot080028, 2014.
[35] S.R. Jaffrey, S.H. Snyder, Sci. STKE 2001 (2001) pl1.
[36] B. Johnsson, S. Lofas, G. Lindquist, Anal. Biochem. 198 (1991) 268–277.
[37] B. Ghebrehiwet, S. Bossone, A. Erdei, K.B. Reid, J. Immunol. Methods 110 (1988) 251–260.
[38] F.T. Ishmael, S.C. Alley, S.J. Benkovic, J. Biol. Chem. 276 (2001) 25236–25242.
[39] S.L. Slatin, A. Nardi, K.S. Jakes, D. Baty, D. Duche, Proc. Natl. Acad. Sci. USA 99 (2002) 1286–1291.
[40] P. Rodríguez-Franco, L. Abad, F.X. Muñoz-Pascual, M. Moreno, E. Baldrich, Sens. Actuators B 191 (2014) 634–642.
[41] P.R. Solanki, S.K. Arya, Y. Nishimura, M. Iwamoto, B.D. Malhotra, Langmuir 23 (2007) 7398–7403.
[42] C. Saby, B. Ortiz, G.Y. Champagne, D. Bélanger, Langmuir 13 (1997) 6805–6813.
[43] X. Liu, Y. Peng, X. Qu, S. Ai, R. Han, X. Zhu, J. Electroanal. Chem. 654 (2011) 72–78.
[44] D. Giustarini, A. Milzani, G. Aldini, M. Carini, R. Rossi, I. Dalle-Donne, Antioxid. Redox Signal. 7 (2005) 930–939.